

Liquid Crystalline Phases in N-(4-n-alkylbenzylidene)-4'-n-alkylanilines

Jürgen Nehring and Maged A. Osman

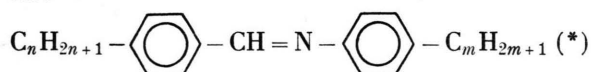
Brown Boveri Research Center and Central Laboratories, CH-5401 Baden, Switzerland

(Z. Naturforsch. 31 a, 786–792 [1976]; received April 14, 1976)

The mesomorphic behavior of N-(4-n-alkylbenzylidene)-4'-n-alkylanilines is investigated and nematic as well as smectic-B phases are found at comparatively low temperatures. Long aliphatic substituents on the aldehyde side of the molecule favor the smectic-B phase. Observations on smectic-B textures, transition enthalpies and density measurements are reported. The simple method used to determine transition temperatures despite impure samples can also be applied to other compounds, e.g. yielding 21.6–47.5 °C for the nematic range of MBBA.

1. Introduction

Several thousand compounds with liquid crystalline phases are presently known¹. According to miscibility criteria eight different types of liquid crystals can be distinguished². For application in electro-optic display devices, nematic liquid crystals with low melting points are especially of interest. In a recent publication³ the synthesis of 34 dialkyl substituted benzylideneanilines of the general structure



with $1 \leq n \leq 7$ and $1 \leq m \leq 6$ has been reported. Some of these substances show liquid crystalline behavior at or below room temperature. In the present paper an account is given of the liquid crystalline phases found in these compounds. For the sake of brevity the substances (*) will be denoted by (n, m) .

2. Experimental Details

All substances were investigated by polarizing microscopy and by differential scanning calorimetry (DSC). The microscope observations were done with a Leitz Orthoplan microscope using a Mettler FP 52 hot-stage for controlled temperature variation. Temperature values below room temperature were obtained by controlled blowing of cold nitrogen gas into the Mettler stage. Above –20 °C, temperatures in the hot-stage were controlled with a Mettler FP 5 temperature control unit whose temperature reading was checked with a calibrated copper-constantan thermocouple which, for this purpose, was placed in the hot-stage at the position where the liquid crystal is normally located. No

Reprint requests to Dr. J. Nehring, Brown Boveri Research Center, CH-5401 Baden, Switzerland.

deviation greater than ± 0.1 °C was observed in the range between room temperature and +60 °C. Below this range the temperature in the stage was determined with the thermocouple immediately after each measurement. In order to confirm that the thermocouple indicated the temperature at the site of the sample, the melting points of ice (0 °C) and p-nitrotoluene (51.6 °C)⁴ were determined several times. The values always coincided with the thermocouple readings within ± 0.1 °C. Temperatures in the range –30 °C to –20 °C were determined with an accuracy of about ± 2 °C. The DSC measurements were carried out on a Perkin Elmer DSC-1B and a DSC-2 Differential Scanning Calorimeter. Densities were measured with a Paar DMA 50 high-precision density meter.

3. Phase Identification

From texture observations under the polarizing microscope two different liquid crystalline phases were found: the nematic and a smectic phase. The nematic phase could easily be identified by its high fluidity, its schlieren texture with $s = 1/2$ singularities⁵ and its threads forming under flow in samples without cover slip. In addition, the typical nematic droplets appeared at the clearing point on cooling from the isotropic phase.

The smectic phase showed high viscosity similar to a wax. No flow could be observed in the bulk, however orientation patterns in thin layers contained between two glass slides were easily changed by shifting the slides with respect to each other. Two characteristic textures were detected: a mosaic texture and a pseudo-isotropic (“homeotropic”) texture. With the latter texture the field of view appeared black for crossed polarizers and in conoscopic observation the uniaxial cross was observed



Dieses Werk wurde im Jahr 2013 vom Verlag Zeitschrift für Naturforschung in Zusammenarbeit mit der Max-Planck-Gesellschaft zur Förderung der Wissenschaften e.V. digitalisiert und unter folgender Lizenz veröffentlicht: Creative Commons Namensnennung-Keine Bearbeitung 3.0 Deutschland Lizenz.

Zum 01.01.2015 ist eine Anpassung der Lizenzbedingungen (Entfall der Creative Commons Lizenzbedingung „Keine Bearbeitung“) beabsichtigt, um eine Nachnutzung auch im Rahmen zukünftiger wissenschaftlicher Nutzungsformen zu ermöglichen.

This work has been digitalized and published in 2013 by Verlag Zeitschrift für Naturforschung in cooperation with the Max Planck Society for the Advancement of Science under a Creative Commons Attribution-NoDerivs 3.0 Germany License.

On 01.01.2015 it is planned to change the License Conditions (the removal of the Creative Commons License condition “no derivative works”). This is to allow reuse in the area of future scientific usage.

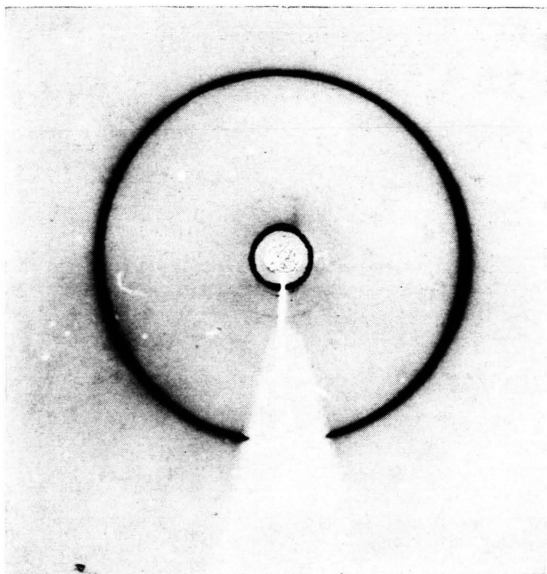


Fig. 1. X-ray diffraction pattern of the smectic-B phase of (7,4) at room-temperature. Monochromatic Cu-K α radiation. Rings correspond to Bragg angles of approximately 1.7° and 10.0°, respectively.



(a)



(b)

Fig. 2. Mosaic smectic-B texture of (5,5) at 29 °C. Crossed polarizers. Polarizers rotated by 40° on going from a to b. Magnification 80 \times .



(a)



(b)

Fig. 3. Mosaic smectic-B texture of (5,5) at 29 °C containing a homeotropic domain (black domain in the center). Crossed polarizers. Polarizers rotated by 20° on going from a to b. Magnification 80 \times .

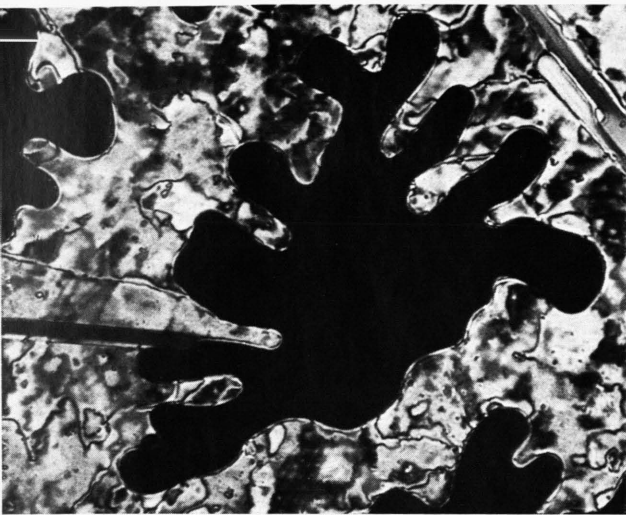


Fig. 4. Homeotropic smectic-B domain growing in the nematic phase of (6,3) at 30.2 °C. Crossed polarizers. Magnification 160 \times .



Fig. 5. Smectic-B crystallites growing in the nematic phase of (5,4) at 24.5°. Crossed polarizers. Magnification 80 \times .

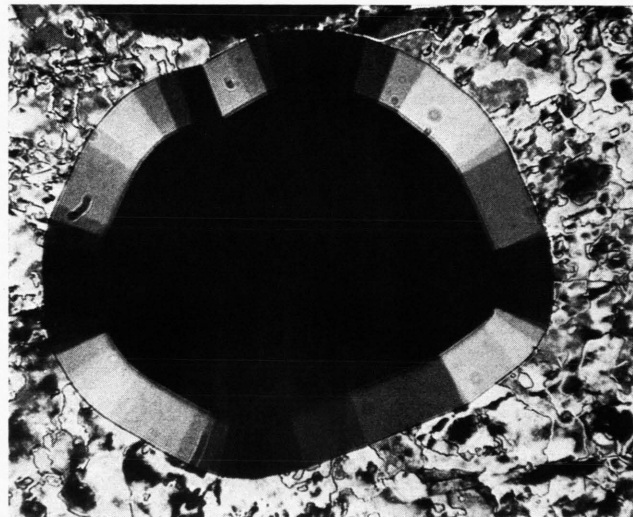


Fig. 7. Smectic-B phase growing around an air bubble in the nematic phase of (6,1) at 16.2 °C. Optic axis in radial direction. Polygonal circumference. Crossed polarizers. Magnification 80 \times .



Fig. 6. Individual smectic-B crystallites with sharp edges and split ends growing in the nematic phase of (4,5) at 6.0 °C. Crossed polarizers. Magnification 160 \times .

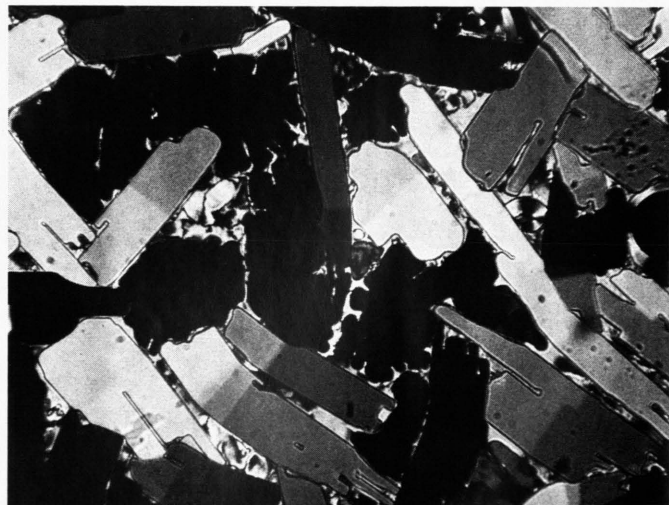


Fig. 8. Nematic gaps of increased impurity concentration separating smectic-B domains in an impure sample of (5,4) at 23 °C. Crossed polarizers. Magnification 80 \times .

in all cases. Stable mosaic textures have been reported⁶ for the smectic phases B, E and G while uniaxiality has been found^{6,7} only in smectic-B and E. In order to distinguish between these two phases⁸, the X-ray diffraction pattern of the smectic phase of compound (7,4) at room temperature was studied (Figure 1*). It shows a sharp inner ring and a sharp outer ring which is characteristic⁸ of smectic-B. Since the temperatures of the smectic/nematic and smectic/isotropic transitions of all investigated compounds show a regular behavior with increasing carbon-chain length and since the textures are the same, we conclude that the smectic phases found in these compounds are all of the smectic-B type.

Textures of solid phases were never affected by shifting the cover slip. Generally sharp-edged crystallites were observed at the solidification and melting points. In some cases, however, this was not possible, especially when the next higher phase was a smectic-B phase. Solidification points were always at least several degrees lower than the melting points, with most substances showing additional solid modifications in the supercooled range. In some substances different solid phases with nearly the same melting point could be identified.

4. Smectic-B Textures

Uniaxial smectic-B phases have a layered structure with the long axes of the molecules perpendicular to the layers and hexagonal packing within the layers². In the homeotropic texture the smectic layers are parallel to the plane of the glass slides between which the liquid crystal is confined. In this case the optic axis is parallel to the sample normal. The mosaic texture consists of different domains, each of which is characterized by a certain optic axis direction⁹. An example of a mosaic texture is shown in Fig. 2 for two different settings of the crossed polarizers. Each domain has a certain color whose brightness and saturation changes continuously when the crossed polarizers are rotated. We denote the plane defined by the sample normal and the optic axis of a domain by p and the angle between p and the extinction direction of one of the crossed polarizers by α . The domain appears black when α is equal to 0° or 90° . For $\alpha = 45^\circ$ the color of the domain has maximum brightness and saturation. A rotation of the crossed polarizers by

$(90^\circ - \alpha)$ does not change the appearance of the domain. The color of neighboring domains, each determined at $\alpha = 45^\circ$, is generally the same, indicating that the angle between the optic axis and the plane of the sample does not change from domain to domain. Knowing the approximate thickness of the sample and the refractive indices of the material it could be estimated from the order of the birefringence colors of the domains that the optic axis lies either in the plane of the sample or is only slightly tilted out of this plane.

It is generally observed that the homeotropic and the mosaic textures occurred in the same sample. In Fig. 3 a mosaic texture is shown containing a homeotropic domain which remained black when the crossed polarizers were rotated. On cooling, the smectic-B phase grew from the nematic or isotropic phase as homeotropic domains (Fig. 4) or as "crystallites" (Figure 5). Consistent with the perpendicular arrangement of the molecules, homeotropic domains had no preferred direction of growth. On the other hand smectic-B crystallites had the shape of rodlets which grew faster in the direction of their long axes. The edges of the rodlets were sharp, but their ends were rounded and had the tendency to split in two (Figure 6). It followed from observation of the dichroism that the optic axis was oriented perpendicular to the long axes of the rodlets. Thus the smectic planes were parallel to the edges of the rodlets which explains their sharpness. The anisotropic growth of the rodlets shows that the smectic-B phase grows faster in the plane of the layers than perpendicular to it. A growth perpendicular to the smectic layers was generally observed around air bubbles (left hand side of Figure 5). The originally smooth circumference of a bubble is transformed into a periphery consisting of straight line segments (Fig. 7) in order to minimize bending of the smectic layers. In contrast to smectic-A layers which are known to bend easily to give focal conic textures, smectic-B layers tend to avoid bending. This explains why no focal conic textures are found in smectic-B phases that grow from a nematic or isotropic phase. While homeotropic domains and crystallites generally form in different parts of the sample, it was also observed that they grow on top of each other, especially if the sample is rapidly cooled. In this case domains arise that have lower order birefringence colors than those usually found in the mosaic texture.

* Figures 1—8 on p. 786 a, b.

It is known that solid crystals growing in the melt tend to exclude impurities. The same observation was made for the smectic-B phase growing in the isotropic or nematic liquid. The impurities accumulate in the gaps between the growing crystallites or homeotropic domains where they lower the transition temperature. In impure samples, several degrees below the transition point to the smectic-B phase, wide isotropic or nematic gaps were seen between the various smectic-B domains (Figure 8).

5. Determination of Transition Temperatures

The purity of the substances as determined by gas-chromatography was generally of the order of 99.5% or better. The main impurities were the aldehyde and the amine from which the specific Schiff's base was made³ and into which it splits by hydrolysis. From a study¹⁰ of N-(4-n-methoxybenzylidene)-4'-butylaniline (MBBA) it is known that 0.5% impurities of the aldehyde or amine type would lower the clearing temperature of a Schiff's base liquid crystal by several degrees. In order to determine the correct temperatures of the clearing and other transition points despite a certain amount of impurity, we used the following simple procedure employing a microscope and a hot-stage. An isotropic or nematic drop of the material was deposited on a glass slide and cooled down to the smectic or solid phase. Then the cover slip was put on so that a wedge-shaped space was formed between the two glasses and the sample was slowly heated in the hot-stage. Flow generally began several degrees below the true transition temperature to the adjacent nematic or isotropic phase, due to the impurity of the material. Because of the wedge-shaped space between the two glass plates, capillary forces directed the flow into the narrow part of the wedge where the impurities accumulated. The pure material was left behind near the position where the substance was originally deposited ("clean spot"). The transition temperatures were determined at the clean spot which in a 1 cm² sample generally comprised an area of several mm². Sharp clearing points were observed at the clean spot. With increasing distance from the clean spot the clearing point became lower and lower and the clearing range broadened. The area of the clean spot was smaller with less pure material and also with faster heating of the sub-

stance. In order to test the method we have determined the correct melting and clearing points of six samples of MBBA containing different amounts of impurities in the range 0.3–2% (clearing points between 47 °C and 39 °C). The results were always the same within ± 0.1 °C:

$$\text{MBBA: cl.p.} = 47.5\text{ }^{\circ}\text{C} \pm 0.1\text{ }^{\circ}\text{C}$$

$$\text{m.p.} = 21.6\text{ }^{\circ}\text{C} \pm 0.1\text{ }^{\circ}\text{C}.$$

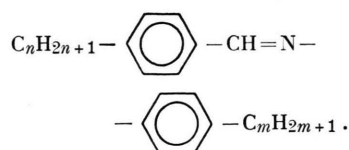
These values fall into the ranges 47–48 °C and 20–22 °C reported in the literature for purified MBBA^{10–13}. (We have also applied this method to a highly contaminated sample of MBBA containing 2% amine and aldehyde and 4% (–)-menthol which was intentionally added to lower the clearing point to about 28 °C. The values obtained were only slightly lower than those for the much purer specimens, namely 47.1 °C and 21.5 °C.)

The transition temperatures of the dialkylbenzylideneanilines are listed in Table 1. Accuracy is generally ± 0.5 °C or better for values given to a tenth of a degree and ± 3 °C for the others. The less accurate values are those of enantiotropic solid/smectic-B transitions and those involving unstable solid modifications. For some of these transitions no sharp texture change could be observed and the transition temperatures were taken from the DSC measurement. Transitions found in the DSC-thermogram which could not be identified with the microscope were not included in Table 1. For some compounds no solidification could be observed at temperatures down to -90 °C and this is indicated in Table 1 by a question mark.

6. Differential Scanning Calorimetry and Density Measurements

Figure 9 shows the DSC-thermograms of (6,1) in the heating and cooling modes measured on a Perkin Elmer DSC-2. The three peaks (a, b, c) refer to the solid/smectic-B, smectic-B/nematic and nematic/isotropic transitions. Only the first of these transitions can be supercooled. For some substances more complicated thermograms were obtained due to the presence of more than one solid phase. In a few cases crystallization was only observed on heating the supercooled melt. The transition enthalpies of the various substances fall into the following ranges:

<i>n</i>	<i>m</i>	K	SB	N	I	additional transitions
1	5	• 33.2		• 19.1*	•	K2 28.8 I
1	6	• 24.6		• 8.5*	•	
2	4	• 6.3		• -8.1*	•	K2 6 I, K3 -15 N
2	5	• 8.2		• 14.2	•	K2 4 N
2	6	• 9.7		• 5.8*	•	K2 7.5 I, K3 -16 N
3	1	• 47.5			•	K2 40 I
3	2	• 22.4			•	
3	3	• 50.5			•	
3	4	• 13.6		• 18.9	•	K2 9 N, K3 4 N
3	5	• 27.1		• 37.0	•	K2 25 N, K3 5 N
3	6	• 0	• 4.9	• 28.9	•	K2 -20 SB
4	2	• 3.9			•	
4	3	• 15.8		• 18.8	•	
4	4	• 17.0		• 10.4*	•	K2 2 N
4	5	• 14.4	• 6.4*	• 26.7	•	
4	6	• 1	• 12.5	• 21.2	•	K2 -20 SB
5	1	• 48.1		• 25.7*	•	
5	2	• -8	• 13.1	• 18.3	•	
5	3	• 23	• 23.3	• 38.0	•	K2 11 SB, K3 7 SB
5	4	• 0	• 25.5	• 30.1	•	
5	5	• 34.5	• 33.3*	• 43.7	•	K2 26 KI
5	6	• -2	• 36.2	• 38.2	•	
6	0	• 15.3	• -19.0*		•	K2 5 I
6	1	• -6	• 16.6	• 18.0	•	
6	2	• ?	• 20.7		•	
6	3	• ?	• 30.7	• 31.5	•	
6	4	• ?	• 30.9		•	
6	5	• 4	• 38.7		•	
6	6	• 10	• 40.2		•	K2 9 SB
7	0	• 9.6	• -11.1*		•	K2 6 I
7	1	• 18	• 28.6	• 33.2	•	K2 0 I
7	2	• 24	• 32.3		•	K2 -19 SB
7	3	• 11	• 44.9		•	
7	4	• ?	• 43.7		•	

Table 1.
Transition temperature (°C) in

Symbols:

K = crystalline, SB = smectic-B, N = nematic, I = isotropic. K2 and K3 denote second and third solid modifications. Dots in columns SB or N indicate that the respective phase exists. Transitions marked with an asterisk are monotropic. Question marks indicate that the material did not freeze on cooling down to -90 °C.

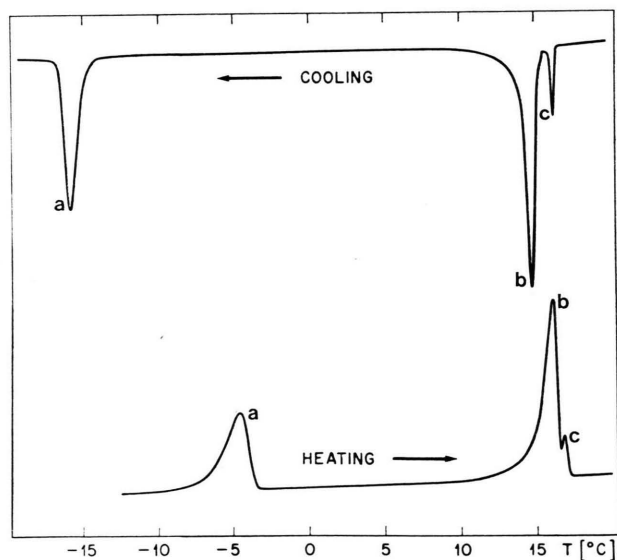


Fig. 9. DSC thermograms of (6,1) taken at heating and cooling rates of 2.5 °C/min. Enthalpies: $\Delta H_a = 0.9$ kcal/mole, $\Delta H_b = 1.2$ kcal/mole and $\Delta H_c = 0.12$ kcal/mole.

nematic/isotropic: 0.05 – 0.3 (kcal/mole),
 smectic-B/isotropic: 1.2 – 1.9 (kcal/mole),
 smectic-B/nematic: 0.6 – 1.3 (kcal/mole),
 melting: 0.9 – 6.2 (kcal/mole).

The nematic/isotropic transition enthalpies are of the same order of magnitude as found in other compounds¹⁴. For smectic-B/isotropic and smectic-B/nematic transitions there are very little data available in the literature. The temperature dependence of the density ρ of (6,5) was measured in order to determine the discontinuity $\Delta\rho$ of a smectic-B/isotropic transition (Figure 10). The value found is $\Delta\rho = 0.02$ (g/cm³). It is of the same order of magnitude as for smectic-B/nematic transitions^{15, 16}.

7. Discussion

The mesomorphic behavior of the dialkylbenzylideneanilines (Table 1) follows the general scheme known from other homologous series. The lower

homologs either are not liquid crystalline at all or are nematic. With increasing alkyl chain length a smectic phase appears in addition to or instead of the nematic phase. Characteristic of these substances are the relatively low melting points leading to mesomorphic phases below room temperature in several cases. The lowest temperature nematic phase, which incidentally also has the broadest range, is found in compound (3,6) with 4.9–28.9 °C. Unusual are also the phase sequences¹ isotropic/smectic-B and nematic/smectic-B. Smectic-B phases are generally followed by other smectic phases (smectic-A or C or both) at higher temperatures¹. The sequence isotropic/smectic-B has so far only been found in very few substances^{17–19}.

It is seen from Table 1 that, within any homologous series of constant aliphatic chain length on either the aldehyde or the amine side, the nematic/isotropic transition points show the usual even-odd alternation². This alternation is caused by the different contributions of even and odd aliphatic carbon-carbon bonds to the anisotropy of the polarizability of the molecules^{20, 21}. Substances with an odd number of carbons in the alkyl chains have therefore higher clearing points than the nearest homologs with an even number of carbon atoms. In

the series (6,m) and (7,m) nematic phases – albeit of very narrow intervals – are only found in the “odd” members (6,1), (6,3) and (7,1). As in other homologous series of low-clearing liquid crystals²², the nematic clearing points increase

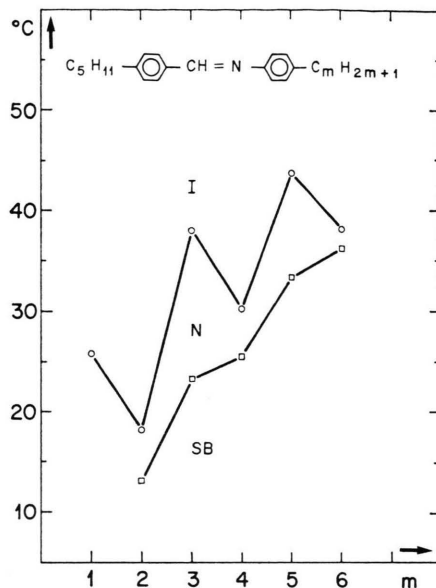


Fig. 11. Isotropic/nematic and nematic/smectic-B transition temperatures in the homologous series (5,m).

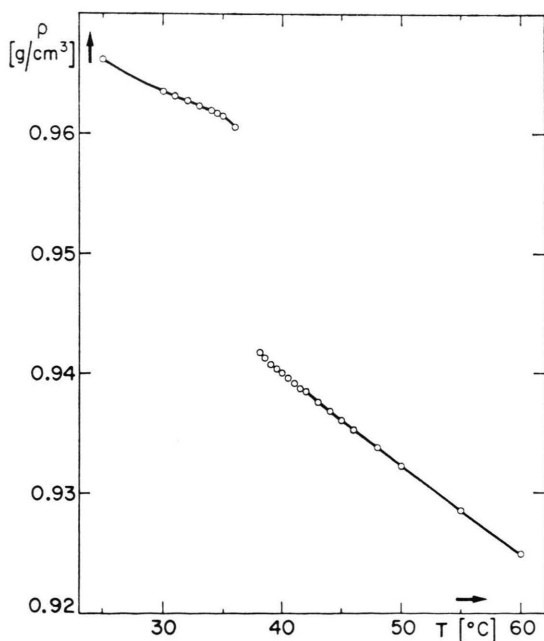


Fig. 10. Temperature dependence of the density ρ of (6,5) in the smectic-B phase and the isotropic phase.

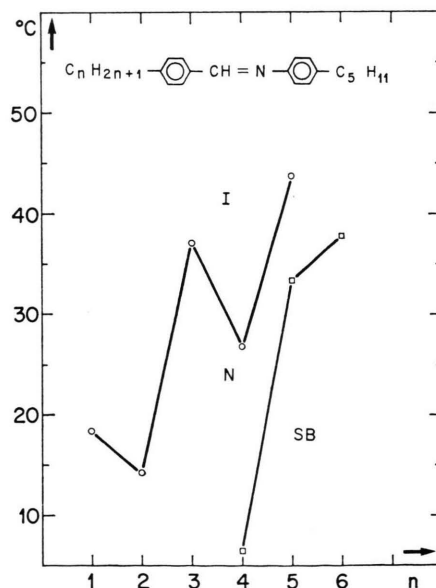


Fig. 12. Isotropic/nematic and nematic/smectic-B transition temperatures in the homologous series (n,5).

Table 2. Comparison of clearing points (cl. p.) and nematic/smectic-B transition temperatures (N/SB) in compounds (n, m) with same total number $n+m$ of aliphatic carbon atoms. Clearing points of smectic-B phases are indicated by a "B". Transitions marked with an asterisk are monotropic.

$n+m$	transition temperatures								
6	(n, m):	(1,5)	(3,3)	(5,1)					
	cl. p.:	19.1*	<39*	25.7*					
	(n, m):	(2,4)	(4,2)						
7	cl. p.:	-8.1*	<0*						
	(n, m):	(1,6)	(2,5)	(3,4)	(4,3)	(5,2)	(6,1)		
	cl. p.:	8.5*	14.2	18.9	18.8	18.3	18.0		
8	N/SB:	<-30*	<-20*	<0*	<10*	13.1	16.6		
	(n, m):	(1,7)	(3,5)	(5,3)	(7,1)				
	cl. p.:		37.0	38.0	33.2				
9	N/SB:		<5*	23.3	28.6				
	(n, m):	(2,6)	(4,4)	(6,2)					
	cl. p.:	5.8*	10.4*	B: 20.7					
10	N/SB:	<-18*	<1*	-					
	(n, m):	(1,8)	(2,7)	(3,6)	(4,5)	(5,4)	(6,3)	(7,2)	(8,1)
	cl. p.:			28.3	26.7	30.1	31.5	B: 32.3	
11	N/SB:			4.9	6.4*	25.5	30.7	-	
	(n, m):	(1,9)	(3,7)	(5,5)	(7,3)	(9,1)			
	cl. p.:			43.7	B: 44.9				
12	N/SB:			33.3*	-				
	(n, m):	(2,8)	(4,6)	(6,4)	(8,2)				
	cl. p.:		21.2	B: 30.9					
13	N/SB:		12.5	-					
	(n, m):	(1,10)	(2,9)	(3,8)	(4,7)	(5,6)	(6,5)	(7,4)	...
	cl. p.:					38.2	B: 38.7	B: 43.7	
14	N/SB:					36.2	-	-	

when C_2H_5 -groups are added to the aliphatic chains. While there is plenty of information in the literature on the behavior of nematic clearing points in homologous series, little is known on transitions involving smectic-B phases. Table 1 shows that isotropic/smectic-B and nematic/smectic-B transitions also show pronounced even-odd alternation. In Figs. 11 and 12 these transition temperatures are plotted against the number of carbon atoms m and n for the complementary series $(5, m)$ and $(n, 5)$. In addition to the even-odd alternation it is noticed that for the lower homologs transition temperatures in $(n, 5)$ are lower and more sensitive to variation of the alkyl chain length than in $(5, m)$. A similar behavior is found for the other complementary series of Table 1.

Additional insight into the tendency of dialkyl substituted benzylideneanilines to form mesomorphic phases is obtained when substances (n, m) with the same total number $t = n + m$ of carbon atoms in the alkyl chains are compared. According

to the mean-field theory of Maier and Saupe²¹, approximately equal nematic clearing points are expected within the group of substances having the same value t provided that t is an odd number. If t is an even number, substances fall into two subgroups with n and m either both even or both odd numbers. Within each subgroup approximately equal nematic clearing points should be found, whereas substances of different subgroups should have different clearing points. In Table 2 clearing points and nematic/smectic-B transitions for $t = 6$ through 11 are given. For some transitions the lowest temperature to which the isotropic or nematic phase could be supercooled with respect to the melting point is given as an upper limit. It follows from Table 2 that for $t = 6$ only monotropic nematic phases are found. For $t > 6$ enantiotropic nematic as well as smectic-B phases occur. As far as can be judged from the limited amount of data assembled in Table 2 the predictions of the Maier-Saupe theory are qualitatively correct except for substances with

very short aliphatic chains on the aldehyde side of the molecule: Nematic clearing points within a given group or subgroup are equal within approximately $\pm 2.5^\circ\text{C}$ except for compounds with methyl substituents on the aldehyde side, whereas the two subgroups belonging to the same (even) value of t differ greatly in their nematic clearing temperatures. Short substituents on the aldehyde side tend to lower the nematic clearing points. There is a strong influence of the alkyl chains on the upper transition temperature T_B of smectic-B phases. It is seen in Table 2 that, within a given group or subgroup,

T_B increases with increasing chain length on the aldehyde side. In two cases — (4,5) and (4,6) — the interchange of the alkyl chains causes an increase of T_B by nearly 20°C . It may be concluded that long alkyl chains on the aldehyde side of the molecule favor the formation of smectic-B phases and thus narrow the nematic range.

Acknowledgement

We are grateful to Dr. T. Hibma for providing us with the X-ray diffraction pattern of (7,4).

- ¹ D. Demus, H. Demus, and H. Zashke, *Flüssige Kristalle in Tabellen*, VEB, Deutscher Verlag für Grundstoffindustrie, Leipzig 1974.
- ² For review see D. Demus, *Z. Chem.* **15**, 1 [1975].
- ³ M. A. Osman, *Z. Naturforsch.* **31b**, (6) [1976].
- ⁴ p-Nitrotoluene was purchased from Fisher Scientific under the trade name "TherMetric Standard T-418-1".
- ⁵ J. Nehring and A. Saupe, *J. Chem. Soc., Faraday Trans. II* **68**, 1 [1972].
- ⁶ H. Sackmann and D. Demus, *Mol. Cryst. Liq. Cryst.* **21**, 239 [1973].
- ⁷ A. Biering, D. Demus, G. W. Gray, and H. Sackmann, *Mol. Cryst. Liq. Cryst.* **28**, 275 [1974].
- ⁸ S. Diele, P. Brand, and H. Sackmann, *Mol. Cryst. Liq. Cryst.* **16**, 105 [1972] and **17**, 163 [1972].
- ⁹ D. Demus, *Wiss. Z. Univ. Halle* **21**, 41 [1972].
- ¹⁰ A. Denat, B. Gosse, and J. P. Gosse, *Chem. Phys. Lett.* **18**, 235 [1973] and *J. Chim. Phys.* **70**, 319 [1973].
- ¹¹ H. Kelker, B. Scheurle, R. Hatz, and W. Bartsch, *Angew. Chem.* **82**, 984 [1970].
- ¹² R. A. Kashnow and H. S. Cole, *J. Appl. Phys.* **42**, 2134 [1971].
- ¹³ G. Brière, R. Herino, and F. Mondon, *Mol. Cryst. Liq. Cryst.* **19**, 157 [1972].
- ¹⁴ D. Marzotko and D. Demus, *Pramana, Suppl. No. 1*, 189 [1975].
- ¹⁵ D. Demus and R. Rurainski, *Z. phys. Chem. Leipzig* **253**, 53 [1973].
- ¹⁶ D. Demus, M. Klapperstück, R. Rurainski, and D. Marzotko, *Z. phys. Chem. Leipzig* **246**, 385 [1971].
- ¹⁷ D. L. Fishel and P. R. Patel, *Mol. Cryst. Liq. Cryst.* **17**, 139 [1972].
- ¹⁸ Chan S. Oh, *Mol. Cryst. Liq. Cryst.* **19**, 95 [1972].
- ¹⁹ D. Demus, L. Richter, C.-E. Rürup, H. Sackmann, and H. Schubert, *J. de Physique* **36**, C1-349 [1975].
- ²⁰ W. Maier and A. Saupe, *Z. Naturforsch.* **12a**, 668 [1957].
- ²¹ W. Maier and A. Saupe, *Z. Naturforsch.* **14a**, 882 [1959].
- ²² W. H. de Jeu and J. van der Veen, *Philips Res. Repts* **27**, 172 [1972].